Cellular Physiology and Biochemistry

Cell Physiol Biochem 2021;55(S3):1-13
DOI: 10.33594/000000335
Published online: 3 March 2021
Accepted: 22 January 2021

Original Paper

Deconstruction – Reconstruction: Analysis of the Crucial Structural Elements of GluN2B-Selective, Negative Allosteric NMDA Receptor Modulators with 3-Benzazepine Scaffold

Nadine Ritter[a,b] Marvin Korff[b,c] Alexander Markus[c] Dirk Schepmann[c] Guiscard Seebohm[a,b] Julian A. Schreiber[a] Bernhard Wünsch[b,c]

[a]Cellular Electrophysiology and Molecular Biology, Institute for Genetics of Heart Diseases (IfGH), Department of Cardiovascular Medicine, University Hospital Münster, Münster, Germany, [b]GRK 2515, Chemical biology of ion channels (Chembion), Westfälische Wilhelms-Universität Münster, Münster, Germany, [c]Institute of Pharmaceutical and Medicinal Chemistry, Westfälische Wilhelms-Universität Münster, Münster, Germany

Key Words
NMDA receptor • GluN2B subunit • Selective GluN2B antagonists • Negative allosteric modulators • Ifenprodil binding site • Deconstruction • Essential structural elements • Reconstruction • Benzoxazolone bioisosteres • Modification of electron density

Abstract
Background/Aims: The NMDA receptor plays a key role in the pathogenesis of neurodegenerative disorders including Alzheimer's and Huntington's disease, as well as depression and drug or alcohol dependence. Due to its participation in these pathologies, the development of selective modulators for this ion channel is a promising strategy for rational drug therapy. The prototypical negative allosteric modulator ifenprodil inhibits selectively GluN2B subunit containing NMDA receptors. It was conformationally restricted as 2-methyl-3-(4-phenylbutyl)-2,3,4,5-tetrahydro-1*H*-3-benzazepine-1,7-diol, which showed high GluN2B affinity and inhibitory activity. For a better understanding of the relevance of the functional groups and structural elements, the substituents of this 3-benzazepine were removed successively (deconstruction). Then, additional structural elements were introduced (reconstruction) with the aim to analyze, which additional modifications were tolerated by the GluN2B receptor. ***Methods:*** The GluN2B affinity was recorded in radioligand receptor binding studies with the radioligand [^{3}H]ifenprodil. The activity of the ligands was determined in two-electrode voltage clamp experiments using *Xenopus laevis* oocytes transfected with cRNA encoding the GluN1-1a and GluN2B subunits of the NMDA receptor. Docking studies showed

Prof. Dr. Bernhard Wünsch
Institut für Pharmazeutische und Medizinische Chemie, Westfälische Wilhelms-Universität Münster, Corrensstraße 48, D-48149 Münster (Germany)
Tel. +49-251-8333311, Fax +49-251-8332144, E-Mail wuensch@uni-muenster.de

the crucial interactions with the NMDA receptor protein. ***Results:*** The deconstruction approach showed that removal of the methyl moiety and the phenolic OH moiety in 7-positon resulted in almost the same GluN2B affinity as the parent 3-benzazepine. A considerably reduced GluN2B affinity was found for the 3-benzazepine without further substituents. However, removal of one or both OH moieties led to considerably reduced NMDA receptor inhibition. Introduction of a NO_2 moiety or bioisosteric replacement of the phenol by a benzoxazolone resulted in comparable GluN2B affinity, but almost complete loss of inhibitory activity. An O-atom, a carbonyl moiety or a F-atom in the tetramethylene spacer led to 6-7-fold reduced ion channel inhibition. ***Conclusion:*** The results reveal an uncoupling of affinity and activity for the tested 3-benzazepines. Strong inhibition of [^{3}H]ifenprodil binding by a test compound does not necessarily translate into strong inhibition of the ion flux through the NMDA receptor associated ion channel. 3-(4-Phenylbutyl)-2,3,4,5-tetrahydro-1*H*-3-benzazepine-1,7-diol (WMS-1410) shows high GluN2B affinity and strong inhibition of the ion channel. Deconstruction by removal of one or both OH moieties reduced the inhibitory activity proving the importance of the OH groups for ion channel blockade. Reconstruction by introduction of various structural elements into the left benzene ring or into the tetramethylene spacer reduced the NMDA receptor inhibition. It can be concluded that these modifications are not able to translate binding into inhibition.

Introduction

Receptors for the amino acid neurotransmitter (*S*)-glutamate are divided into metabotropic G protein-coupled receptors and ionotropic receptors ((*S*)-glutamate gated ion channels). The group of ionotropic glutamate receptors consists of AMPA, kainate and NMDA receptors. These receptors are named according to their prototypical agonists α-amino-(3-hydroy-5-methylisoxazol-4-yl)propionic acid (AMPA), kainic acid (kainate) and *N*-methyl-D-aspartate (NMDA) [1-4].

The NMDA receptor is characterized by four special features: (1) Two agonists are required to open the ligand gated ion channel. (*S*)-Glutamate has to bind to its binding site at the GluN2 subunit and simultaneously glycine has to bind to the glycine-binding site on the GluN1 subunit. (2) At normal membrane potential, Mg^{2+}-ions are bound within the ion channel pore inhibiting the ion flux through the ion channel. Prior to ion channel opening, the Mg^{2+}-ions have to be removed by depolarization of the surrounding membrane. (3) The NMDA receptor controls the penetration of Ca^{2+}-ions into the neuron, which are responsible for the activation of several following Ca^{2+}-dependent processes, including long term potentiation and excitotoxicity. (4) The NMDA receptor has several binding sites for ligands. These binding sites are located in the transmembrane domain (PCP binding site, binding site for Mg^{2+} ions), the ligand-binding domain (glutamate and glycine binding sites) and the amino-terminal domain (binding sites for NO, H^+, Zn^{2+}, polyamines, ifenprodil). Opening of the NMDA receptor can be modulated by various ligands interacting with these binding sites [1-4].

Acute elevated Ca^{2+}-concentrations resulting from excessive NMDA receptor opening are responsible for excitotoxic processes, i.e. processes leading to neuronal cell damage upon release of the excitatory neurotransmitter (*S*)-glutamate. These neurotoxic effects followed by apoptosis are involved in acute traumatic brain injury, intoxications, ischemic processes and stroke. They also play a crucial role in the pathogenesis of chronic neurodegenerative disorders such as Alzheimer's, Parkinson's and Huntington's disease as well as depression and alcohol or drug dependence [5-10].

For a better understanding of the NMDA receptor function, its structure has to be analyzed carefully. The NMDA receptor consists of four subunits, usually two GluN1 and two GluN2 subunits. Whereas only one gene encoding the GluN1 subunit is known, four genes encode for the four GluN2A-D subunits. The GluN3A and GluN3B subunits are predominantly expressed in the pre- and perinatal phase and are therefore no further considered herein [11-13].

In 2011, X-ray crystal structures of a dimer of the amino terminal domains (ATD) of the GluN1b splice variant and the GluN2B subunit cocrystalizied with ifenprodil and Ro 25, 6981 were reported [14]. Three years later, the first structure of the complete NMDA receptor containing two GluN1b and two GluN2B subunits was released. In this X-ray crystal structures, the intracellularly located carboxy terminal domain (CTD) connecting the receptor with the cytoskeleton is missing [15, 16]. Additionally, recent cryo EM structures depicting the ion channel in the open (active form, PDB 5FXG) and closed state (deactivated form, PDB 5FXI) have been reported [17].

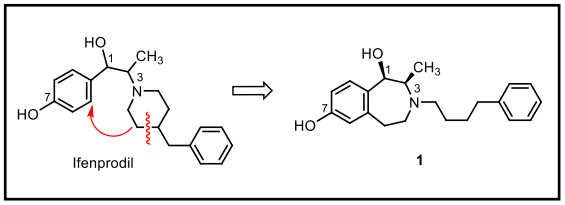

Fig. 1. Development of tetrahydro-3-benzazepine **1** by formal rearrangement of ifenprodil. Ifenprodil and **1** are constitutional isomers.

The prototypical ligand for NMDA receptors containing the GluN2B subunit is ifenprodil [18-20], which interacts with a binding site at the interface between the GluN1 and GluN2B subunit in the ATD (ifenprodil binding site). Formal rearrangement of ifenprodil by cleavage of a piperidine ring bond and reconnecting this bond to the benzene ring leads to tetrahydro-3-benzazepine **1** (see Fig. 1). Recently, we have reported the synthesis and pharmacological evaluation of **1** and its stereoisomers as potent and selective negative allosteric modulators of NMDA receptors containing the GluN2B subunit, even exceeding inhibitory activity of ifenprodil. **1** interacts with the ifenprodil binding site within the ATD [21].

The aim of this project is the analysis of the structural elements of the 3-benzazepine-based GluN2B antagonist **1**, which are crucial for high GluN2B affinity, inhibition of the associated ion channel and receptor selectivity. At first, a deconstruction approach was pursued leading to less substituted compounds. Then, additional substituents and structural elements were attached to the 3-benzazepine scaffold leading to more complex compounds (reconstruction approach).

Materials and Methods

Synthesis of compound 7

cis-/trans-9-Hydroxy-7-(4-phenylcyclohexyl)-3,5,6,7,8,9-hexahydrooxazolo [4,5-h]-[3]benzazepin-2-one (7)

*cis-/trans-**12*** [22] (140 mg, 0.34 mmol) was dissolved in EtOH (4 mL) and conc. HCl (42 µL, 0.5 mmol) was added. A solution of $RhCl_3 \cdot 3\ H_2O$ (9 mg, 0.034 mmol) in EtOH (1 mL) was added dropwise. The solution was stirred at 90 °C for 2 h before the solvent was removed under reduced pressure. To the crude intermediate 4 M HCl (12 mL) was added and stirring was continued for 3 h at 100°C. Then 10 M NaOH and at the end saturated $NaHCO_3$ solution were added until pH 7 followed by extraction with ethyl acetate (3x). The combined organic layers were dried (Na_2SO_4) and the solvent was removed under reduced pressure giving a brown oil as crude product, which was purified by flash column chromatography (Ø 2 cm, 19 cm, ethyl acetate: n-hexane 4 : 1 + 1 % *N*,*N*-dimethylethanamine, fraction size 10 mL, R_f = 0.12). Colorless crystals, mp 120 °C, yield 40.4 mg (32 %). $C_{23}H_{26}N_2O_3$ (M_r = 378.5). ^{1}H NMR (CD_3OD): δ [ppm] = 1.56 – 1.71 (m, 4H, 3-H / 5-$H_{cyclohexane}$), 1.75 – 1.89 (m, 2H, 2-H / 6-$H_{cyclohexane}$), 1.97 – 2.10 (m, 2H, 2-H / 6-$H_{cyclohexane}$), 2.45 – 2.64 (m, 2H, 8-H / 6-H), 2.68 – 2.74 (m, 1H, 1-$H_{cyclohexane}$), 2.75 – 2.83 (m, 1H, 4-$H_{cyclohexane}$), 2.88 – 2.97 (m, 3H, 8-H / 6-H / 5-H), 3.02 (d, J = 12.3 Hz, 1H, 5-H), 4.80 (d, J = 11.1 Hz, 1H, 9-H), 6.83 (s, 1H, 4-H), 7.17 – 7.26 (m, 5H, -CH-C_6H_5), 7.28 (s, 1H, 10-H). Signals for the OH- and NH-protons are not seen in the ^{1}H NMR-spectrum. MS (EI): m/z (%) = 378 (M, 15), 360 (M – H_2O, 16), 91 (Benzyl, 13). Purity (HPLC): 98.3 % (cis + trans), t_R = 16.1 min (cis-isomer), 16.5 min (trans-isomer). IR (neat): $\tilde{\nu}$ [cm^{-1}] = 3412 (m, ν_{O-H}), 2932 (m) / 2861 (w, $\nu_{C-H\ aliph.}$), 1743 (s, $\nu_{C=O\ oxazolone}$), 1620 (w) / 1489 (s, $\nu_{C=C\ arom.}$), 759 (s) / 698 (s, $\gamma_{monosubst.\ arom.}$).

Radioligand receptor binding studies

The affinity towards the ifenprodil binding site of GluN2B subunit containing NMDA receptors was recorded as described in references [23, 24]. Performance of the σ_1 and σ_2 assays is reported in references [25-27]. The corresponding procedures are given in the Supporting Information (for all supplementary material see www.cellphysiolbiochem.com).

GluN2B binding assay. The competitive binding assay was performed with the radioligand [^{3}H]ifenprodil (60 Ci/mmol; BIOTREND, Cologne, Germany). The thawed cell membrane preparation from the transfected L(tk-) cells (about 20 µg protein) was incubated with various concentrations of test compounds, 5 nM [^{3}H] ifenprodil, and TRIS/EDTA-buffer (5 mM TRIS/1 mM EDTA, pH 7.5) at 37°C. The non-specific binding was determined with 10 µM unlabeled ifenprodil. The K_d value of ifenprodil is 7.6 nM [23].

σ_1 receptor assay. The assay was performed with the radioligand [^{3}H]-(+)-pentazocine (22.0 Ci/mmol; Perkin Elmer). The thawed membrane preparation of guinea pig brain (about 100 µg of the protein) was incubated with various concentrations of test compounds, 2 nM [^{3}H]-(+)-pentazocine, and TRIS buffer (50 mM, pH 7.4) at 37 °C. The non-specific binding was determined with 10 µM unlabeled (+)-pentazocine. The K_d value of (+)-pentazocine is 2.9 nM [28].

σ_2 receptor assay. The assays were performed with the radioligand [^{3}H]di-*o*-tolylguanidine (specific activity 50 Ci/mmol; ARC, St. Louis, MO, USA). The thawed rat liver membrane preparation (about 100 µg protein) was incubated with various concentrations of the test compound, 3 nM [^{3}H]di-*o*-tolylguanidine and buffer containing (+)-pentazocine (500 nM (+)-pentazocine in TRIS buffer (50 mM TRIS, pH 8.0)) at rt. The non-specific binding was determined with 10 µM non-labeled di-*o*-tolylguanidine. The K_d value of di-*o*-tolylguanidine is 17.9 nM [29].

Two-electrode voltage clamp experiments

Molecular biology and oocyte preparation. cRNA of GluN2B/pSGEM and GluN1-1a/pSGEM was generated as previously described [30]. In brief, *in vitro* transcription was performed using mMessage mMaschine T7 kit (Life Technologies, Darmstadt, Germany) and linearized cDNA constructs (PacI for GluN1-1a, NheI for GluN2B). Defolliculated oocytes were purchased from EcoCyte Bioscience (Dortmund, Germany) and injected with 0.8 ng GluN1-1a and 0.8 ng GluN2B cRNA per oocyte using a nanoliter injector 2000 (WPI, Berlin, Germany). After injection, oocytes were incubated for 5 d at 18 °C in Barth's solution, containing (mmol L^{-1}): 88 NaCl, 1 KCl, 0.4 $CaCl_2$, 0.33 $Ca(NO_3)_2$, 0.6 $MgSO_4$, 5 TRIS-HCl, 2.4 $NaHCO_3$, supplemented with 80 mg L^{-1} theophylline, 63 mg L^{-1} benzylpenicillin, 40 mg L^{-1} streptomycin, and 100 mg L^{-1} gentamycin.

Compound solutions and TEVC-recordings. The TEVC experiments were conducted as previously described [30]. All compounds were provided as 10 mM stock solutions in DMSO. The compounds were diluted with agonist solution and adjusted to 0.1% DMSO concentration. Agonist solution was freshly prepared by adding 10 µM glycine and 10 µM (*S*)-glutamate to barium ringer solution containing 10 mM HEPES, 90 mM NaCl, 1 mM KCl and 1.5 mM $BaCl_2$ (adjusted to pH 7.4 by NaOH). The inhibitory activity was measured via TEVC in *X. laevis* oocytes at room temperature with a holding potential of -70 mV using a Turbo Tec 10CX amplifier (NPI electronic, Tamm, Germany), NI USB 6221 DA/AD Interface (National Instruments, Austin, USA) and GePulse Software (Dr. Michael Pusch, Genova, Italy). Electrodes were backfilled with 3 M KCl and had resistances between 0.5 and 1.5MΩ. The compounds were tested by applying ascending concentrations in presence of the agonists, ranging from 1 up to 30,000 nM, in at least six oocytes. In Fig. 2, an example for the current trace of GluN1-1a/GluN2B expression oocytes is shown.

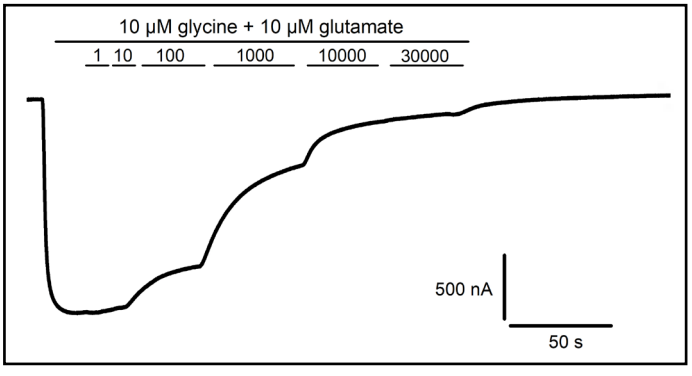

Fig. 2. Example current trace of GluN1-1a/GluN2B expressing oocytes. After activation by 10 µM glycine and 10 µM (S)-glutamate the receptor was inhibited by ascending inhibitor concentrations, ranging from 1 up to 30,000 nM. The typical curve recorded with fluoro derivative **10** is shown exemplarily.

Docking and statistical evaluation

Docking procedures and statistical evaluation were previously described and adapted from publication Schreiber et al. [30].

Results

Deconstruction

The affinity towards the ifenprodil binding site of NMDA receptors containing the GluN2B subunit (GluN2B affinity) was determined in radioligand receptor binding studies. L(tk-) mouse fibroblast cells stably expressing the GluN1-1a and GluN2B subunits served as receptor material. These cells were used to prepare a membrane preparation by homogenization. Tritium labeled [^{3}H]ifenprodil was employed as competitive radioligand [23, 24].

The inhibitory activity at GluN2B receptors was recorded in two-electrode voltage clamp (TEVC) experiments. cRNA encoding for the GluN1-1a and GluN2B subunits was injected into oocytes of *Xenopus laevis*. After production of functional NMDA receptors, the oocytes were treated with (*S*)-glutamate and glycine and later with different concentrations of the test compounds. The current necessary to compensate the resulting ion flux was measured by two electrodes injected into the oocytes [30]. A prototypical current trace is depicted in Fig. 2 in the Materials and Methods part.

Formal rearrangement of ifenprodil resulted in the tetrahydro-3-benzazepine **1**, which represents a constitutional isomer of ifenprodil [21] (Fig. 3). Although the binding affinity of **1** (K_i = 111 nM) is lower than the binding affinity of ifenprodil (K_i = 10 nM), its inhibitory activity at GluN2B subunit-containing NMDA receptors is 3-fold higher (IC_{50} = 91 nM versus 264 nM) [21, 30] (Table 1).

In Fig. 4 the binding mode of ifenprodil redocked into the X-ray crystal structure of the GluN2B-NMDA receptor is shown (PDB 4PE5). Several H-bond interactions as well as aromatic interactions are detectable. The phenolic OH moiety forms an H-bond interaction with the carboxylate moiety of Glu236 from the GluN2B subunit, while the benzylic OH moiety interacts with the backbone carbonyl moiety of Ser132 from the GluN1 subunit. The protonated amino moiety reacts as H-bond donor with the C=O moiety of Gln110. In addition to these H-bonds two strong aromatic interactions with Phe114 and Phe176 from the GluN2B subunit can be seen. In particular, the interaction of ifenprodil with Phe176 is important, as the negative allosteric modulator inhibits the backward movement of this amino acid, which is needed for the transition from closed to open state (Foot-in-the-door mechanism) [30].

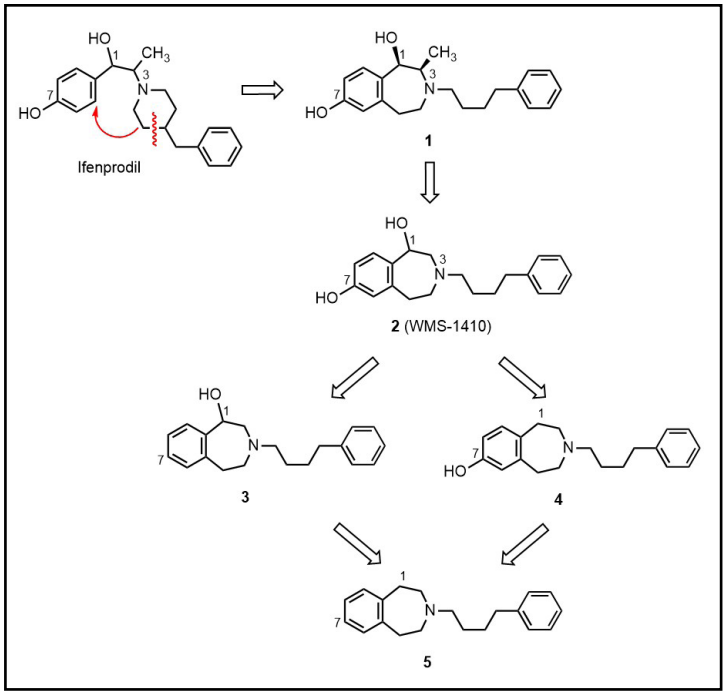

Fig. 3. Ifenprodil as starting point for the development of tetrahydro-3-benzazepine **1** and deconstruction of **1** by stepwise removal of the methyl moiety as well as the phenolic and benzylic OH moieties.

Table 1. Receptor affinity and activity of ifenprodil and tetrahydro-3-benzazepines **1-5**. n.d. = not determined; $The given IC_{50} values result from measurements of 18 – 30 oocytes, respectively; #Due to low GluN2B inhibitory activity, the inhibition (in % ± SEM) at a test compound concentration of 30 µM is given

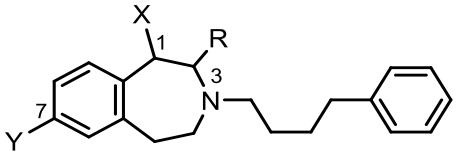

1 - 5

compd.	X	Y	R	K_i ± SEM [nM] (n=3) GluN2B	IC_{50} ± SE [nM]$ GluN2B	K_i ± SEM [nM] (n=3) σ_1	σ_2
ifenprodil	-	-	-	10 ± 0.7	264 ± 27	125 ± 24	98 ± 34
1	OH	OH	CH_3	111 ± 53	91 ± 7	85 ± 3	148 ± 11
2 (WMS-1410)	OH	OH	H	84 ± 18	94 ± 8	123	32 ± 13
3	OH	H	H	73 ± 2	n.d.	676	76 ± 26
4	H	OH	H	9.9 ± 2.7	3367 ± 926	32 ± 8	12 ± 3
5	H	H	H	225 ± 2	9 ± 2%#	10 ± 8	35 ± 13

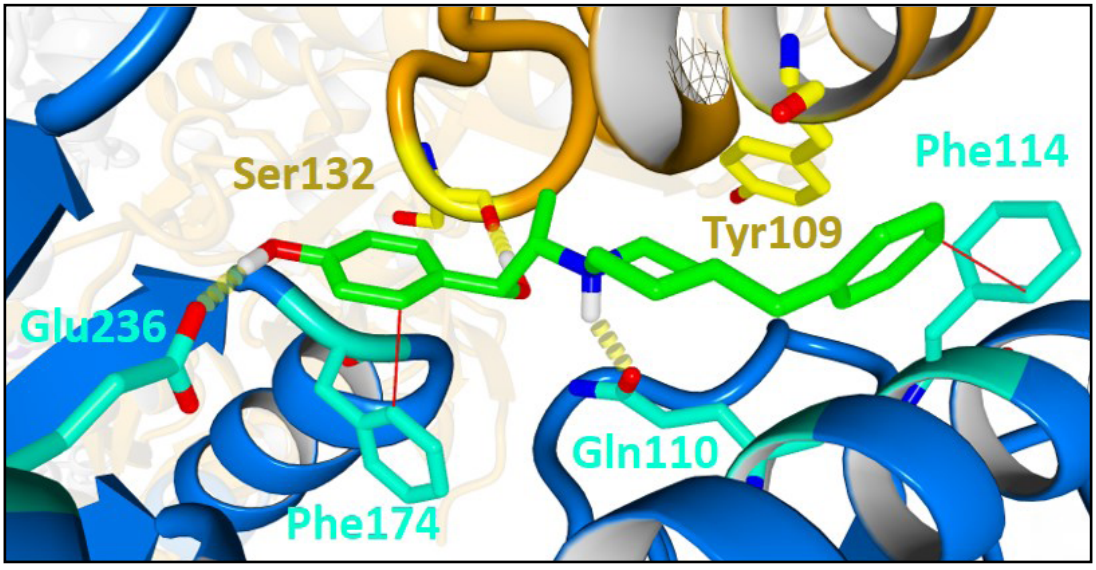

Fig. 4. Ifenprodil (green) re-docked into the X-ray crystal structure of the tetrameric GluN1 (orange) / GluN2B (blue) NMDA receptor (PDB 4PE5). H-bond interactions with Ser132 (yellow) from GluN1 as well as H-bond interactions with GluN2B residues Gln110 (cyan) and Glu236 (cyan) marked by yellow dashed lines. Aromatic interactions with Phe114 (cyan) and Phe176 (cyan) are shown by red lines.

Docking of the 3-benzazepine **1** into the ifenprodil binding pocket resulted in nearly the same crucial interactions except the H-bond with Ser132 (Fig. 5). Additionally, to the two previous detected aromatic interactions, a weak aromatic interaction with Tyr109 from the GluN1 subunit can be seen.

In order to analyze the importance of the different substituents and functional groups, the substituents of **1** were removed successively. At first the methyl moiety of **1** was eliminated leading to the 3-benzazepine-1,7-diol **2** (WMS-1410, Fig. 3), with only one center of chirality [31]. WMS-1410 (**2**) showed a slightly increased affinity towards GluN2B-NMDA

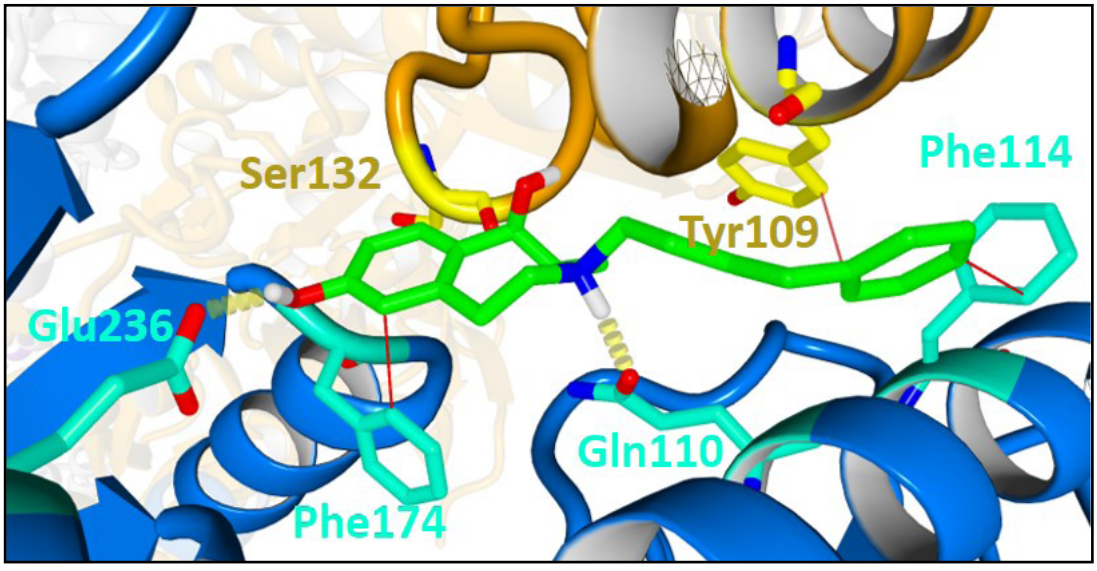

Fig. 5. Interactions of tetrahydro-3-benzazepine **1** (green) after docking into the X-ray crystal structure of the tetrameric GluN1b (orange) / GluN2B (blue) NMDA receptor (PDB 4PE5). H-bond interactions are shown as yellow dashed lines, while aromatic interactions are depicted by red lines.

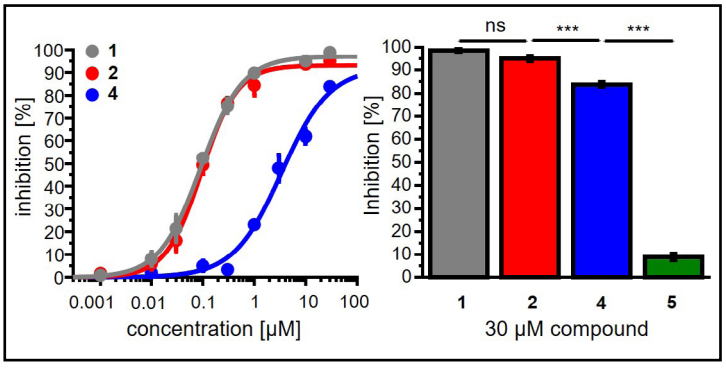

Fig. 6. Left: Dose-response curves derived from inhibition of GluN1-1a/GluN2B expressing oocytes at ascending concentrations of compounds **1** (gray), **2** (red) and **4** (blue). The holding potential was set to -70 mV and the receptors were activated by 10 µM glycine and 10 µM (S)-glutamate. Right: inhibition (% ± SEM) of 30 µM **1**, **2**, **4** and **5** at GluN1/GluN2B expressing oocytes. Significance of mean differences was tested by one-way ANOVA with post hoc mean comparison Tukey test (*** $p<0.001$; ns $p > 0.05$).

receptors (K_i = 84 nM (**2**) versus 111 nM (**1**), see Table 1). A further slight increase of GluN2B-NMDA receptor affinity was achieved by elimination of the phenolic OH moiety (K_i = 73 nM (**3**) [32] versus 84 nM (**2**)), but removal of the benzylic OH moiety resulted in a strong increase of the GluN2B-NMDA receptor affinity (**4**, K_i = 9.9 nM) [33]. Unexpectedly, even the naked compound **5** without CH_3 and OH moieties exhibited moderate GluN2B affinity (K_i = 225 nM) [32] (Fig. 3). It can be concluded that the phenolic OH moiety is essential for high binding at the ifenprodil binding site of the GluN2B-NMDA receptor (Fig. 3, Table 1).

Compared to ifenprodil (IC_{50} = 264 nM), the rearranged 3-benzazepine-1,7-diols **1** and **2** showed a 3-fold increased inhibition of the ion channel (IC_{50} = 91 nM and 94 nM) [30] (Fig. 6). The similar activity of **1** and **2** correlates nicely with their similar affinity. However, ifenprodil itself showed a considerably higher GluN2B affinity (K_i = 10 nM), but reduced activity (IC_{50} = 264 nM). A similar behavior shows the phenol **4** without benzylic OH moiety. In the affinity assay it exhibits low nanomolar affinity (K_i = 9.9 nM), but its channel inhibition is rather low (IC_{50} = 3367 nM). The moderate GluN2B affinity of the "naked" 3-benzazepine **5** translates in low activity in the TEVC experiment. Even at test compound concentration

of 30 μM, **5** could only slightly inhibit (<10 %) the ion flux stimulated by the agonists (*S*)-glutamate and glycine. Obviously, for some compounds a direct correlation between binding affinity and inhibitory activity does not exist.

As ifenprodil was described as σ receptor ligand as well, the σ_1 and σ_2 affinity of the 3-benzazepines **1** – **5** was recorded in radioligand receptor binding studies [25-27]. The σ_1 and σ_2 affinity of the 3-benzazepines **1** - **4** is in the same range as their GluN2B affinity. The only exceptions from this rule are the σ_1 affinities of monohydroxylated ligands **3** and **4**, which are 10- and 3-fold lower than their GluN2B affinity, respectively. The 3-benzazepine **5** without further substituents at the 3-benzazepine scaffold shows 22-fold and 6-fold preference for σ_1 and σ_2 receptors, respectively. It can be concluded that removal of polar substituents favors the interactions with σ_1 and σ_2 receptors. The synthesis of the 3-benzazeines **1**-**5** has already been reported in literature [21, 31-33].

Reconstruction

After having identified the substituents and functional groups of 3-benzazepine **2** (WMS-1410), which are crucial to achieve high receptor affinity and strong inhibition of the ion channel, the effect of further decoration of the tetrahydro-3-benzazepine-1,7-diol system should be investigated. This reconstruction approach is displayed in Fig. 7.

In a first approach, the phenol of **2** was replaced by a nitrophenyl moiety (**6**) [32]. Replacement of the OH moiety by a NO_2 group changes the electronic nature of the central benzene ring, i.e. the electron rich benzene ring of **2** is changed into an electron deficient benzene ring in **6**. In contrast to the OH moiety, the NO_2 moiety can only react as H-bond acceptor, but not as H-bond donor, which weakens the interaction with Glu236 (see Fig. 5). In receptor binding studies, the NO_2 derivative **6** exhibited 5-fold higher GluN2B affinity (K_i = 16 nM) than the phenol **2** (WMS-1410). Unexpectedly, this high affinity did not translate into strong ion channel inhibition, as **6** could not inhibit the ion flux in the TEVC experiment up to a concentration of 1 μM (Table 2).

Due to fast biotransformation, the phenol does not represent a first-choice functional group in drugs. In particular, ifenprodil and **2** (WMS-1410) can be fast conjugated with glucuronic acid upon incubation with mouse liver microsomes [34-36]. Therefore, the phenol of **2** was replaced bioisosterically by a benzoxazolone system (**7**). This approach had been successfully applied during the development of besonprodil [37]. Although the GluN2B affinity of benzoxazolone **7** is in the same range as the GluN2B affinity of phenol **2**, its channel blocking activity is rather low. At a test compound concentration of 1 μM **7** showed only 15 % inhibition of the ion channel.

In compounds **8** and **9** the polarity of the tetramethylene spacer and the electron density of the terminal phenyl moiety were modified. Whereas the electron density of the terminal phenyl moiety in the ether **8** is increased, the phenyl ring in the ketone **9** has reduced electron density The F-atom in *p*-position of **9** further reduces the electron density of the terminal phenyl moiety. Compared to the lead compound **2** (WMS-1410) with a 4-phenylbutyl side chain, the ether **8** displays lower GluN2B affinity (K_i = 219 nM) and the ketone **9** shows higher GluN2B affinity (K_i = 36 nM). However, both compounds **8** and **9** were less potent in the TECV experiment and revealed almost the same low IC_{50} values of 674 nM and 778 nM, respectively. The modified electron density of the terminal phenyl moiety influences considerably the GluN2B affinity, but not the ion channel inhibition (Fig.8).

The last modification comprises the introduction of a F-atom into the γ-position of the side chain (**10**), which reduces the basicity of the 3-benzazepine system [33]. Whereas the GluN2B affinity of **10** is approximately 10-fold lower than that of the ketone **9**, their inhibitory activities are comparable (Fig. 8). The potentially reduced basicity of **10** does not reduce the ion channel inhibitory activity.

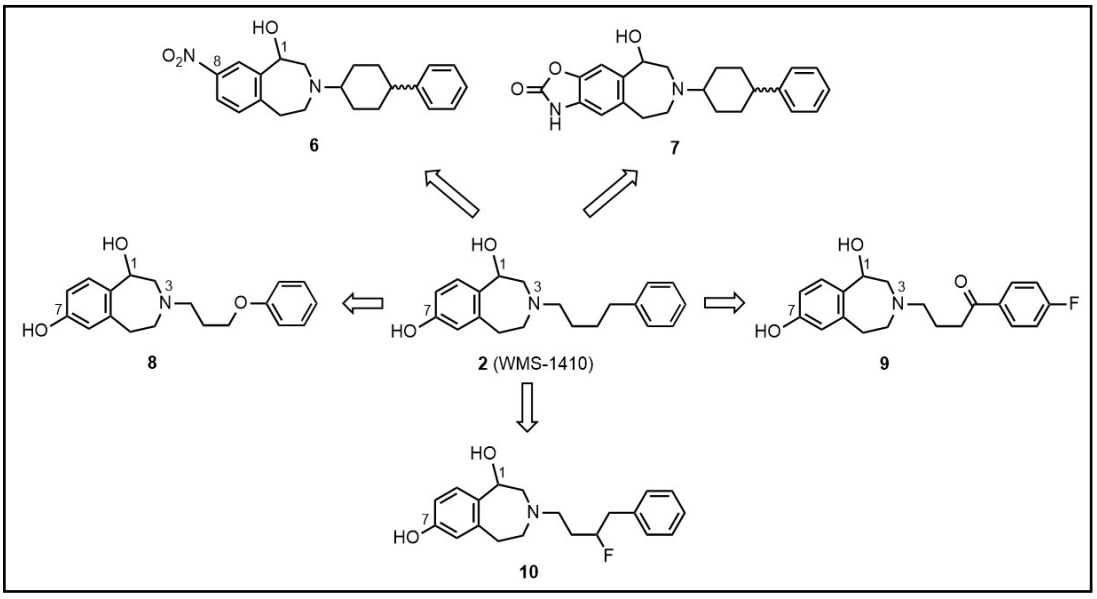

Fig. 7. Reconstruction of WMS-1410 (**2**): A NO_2 moiety was introduced in 8-position instead of the 7-OH-moiety (**6**). The phenol was replaced bioisosterically by a benzoxazolone system (**7**). An O-atom (**8**), a carbonyl moiety (**9**) and an F-atom (**9**, **10**) were introduced into the 4-phenylbutyl side chain.

Table 2. Receptor affinity and activity of ifenprodil and WMS-1410 (**2**) and tetrahydro-3-benzazepines **6** - **10**. #Due to low GluN2B inhibitory activity, the inhibition of ion flux (in %) at a test compound concentration of 1 µM is given

compd.	K_i ± SEM [nM] (n=3)	IC_{50} ± SE [nM] (n=3)	K_i ± SEM [nM] (n=3)	
	GluN2B	GluN2B	σ_1	σ_2
ifenprodil	10 ± 0.7	264 ± 27	125 ± 24	98 ± 34
2 (WMS-1410)	84 ± 18	94 ± 8	123	32 ± 13
6	16 ± 2	5 ± 3%#	360	24 ± 4
7	114	15 ± 6%#	265	996
8	219	574 ± 95	170 ± 51	5.9 ± 1.7
9	36 ± 6	778 ± 142	1100	34 ± 12
10	422	496 ± 316	1400	130 ± 26

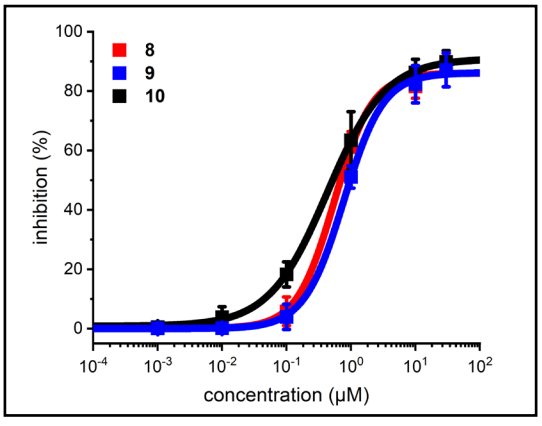

Fig. 8. Dose-response curves derived from inhibition of GluN1-1a/GluN2B expressing oocytes at ascending concentrations of compound **8** (red), **9** (blue) and **10** (black), respectively. The holding potential was set to -70 mV and the receptors were activated by 10 µM glycine and 10 µM glutamate.

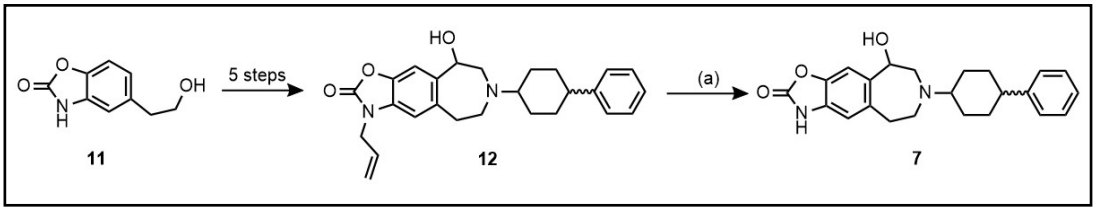

Fig. 9. Outline of the synthesis of the benzoxazolone bioisostere **7**. Reagents and reaction conditions: (a) $RhCl_3 \cdot 3\ H_2O$, EtOH, HCl, 90°C, 2 h; yield 32 % [22].

Although the σ_1 affinity is not negligible, ligands **8 – 10** with modified side chain display lower σ_1 affinity than ifenprodil and WMS-1410 (**2**). However, with exception of the benzoxazolone **7** and the ketone **10**, the ligands **6**, **8** and **9** show very high σ_2 affinity with K_i values in the range 5.9 – 34 nM. Considering only the K_i values, only the benzoxazolone **7** has a selectivity for GluN2B receptors over σ_2 receptors. The NO_2 derivative **6** and the ketone **9** have almost the same affinity towards both GluN2B and σ_2 receptors. The ether **8** and the fluoro derivative **10** exhibit high and moderate selectivity for σ_2 receptors over GluN2B receptors, respectively. Comparing the GluN2B activity with the σ_2 affinity results in high selectivity for σ_2 receptors over GluN2B receptors. However, this selectivity has to be evaluated very critically, as activity data and affinity data are compared.

Whereas the synthesis of **6** and **8**-**10** has been reported in literature, the synthesis of the benzoxazolone bioisostere **7** is outlined in Fig. 9 [22]. Starting with the alcohol **11**, the tricyclic ring system of **12** was established by Mitsunobu reaction, introduction of the allyl protective group, intramolecular Friedel-Crafts acylation and introduction of the N-substituent. In the critical last step, the allyl protective group of **12** was removed by Rh-catalyzed double bond isomerization and subsequent hydrolysis [38, 39]. The benzoxazolone **7** without a substituent at the benzoxazolone-N-atom was obtained in 32 % yield.

Discussion

The formal rearrangement of ifenprodil, the prototypical negative allosteric modulator at GluN2B subunit-containing NMDA receptors, led to the constitutional isomer 3-benzazepine **1**. The transformation of ifenprodil into 3-benzazepine **1** resulted in decreased GluN2B affinity, but increased GluN2B inhibitory activity and selectivity over related σ_1 and σ_2 receptors. The GluN2B binding affinity was measured in a competitive binding assay with the radioligand [^{3}H]ifenprodil and the inhibitory activity was recorded by TEVC experiments using oocytes expressing GluN1 and GluN2B subunits of the NMDA receptor. The missing correlation between affinity and inhibitory activity at GluN2B receptors is an important feature observed for this 3-benzazepine class of negative allosteric modulators.

During the deconstruction process, structural features of **1** were eliminated step-by-step to identify crucial structural elements essential for high GluN2B affinity and inhibitory activity. Removal of the CH_3 group of **1** led to an almost unchanged biological profile of WMS-1410 (**2**). Further removal of the benzylic and phenolic OH moieties resulted in significantly decreased activity at GluN2B receptors as well as reduced selectivity over σ_1 and σ_2 receptors. It is implied that the presence of polar substituents such as a phenolic and benzylic OH group favors the GluN2B inhibitory activity. Furthermore, the absence of these polar groups led to increased σ_1 and σ_2 receptor affinities, i.e. reduced selectivity for GluN2B receptors over σ receptors.

The reconstruction approach was based on WMS-1410 (**2**). On the one side, structural features identified as essential were replaced bioisosterically resulting in NO_2-substituted 3-benzazepine **6** (OH / NO_2 exchange) and benzoxazolone **7** (phenol / benzoxazolone exchange). On the other side, additional structural elements were introduced into the tetrahydro-3-benzazepine-1,7-diol **2** including an O-atom (**8**) and a carbonyl moiety (**9**) in

the tetramethylene linker as well as an F-atom in the terminal phenyl moiety (**9**) and the tetramethylene linker (**10**). As the 4-phenylcyclohexyl moiety replacing the 4-phenybutyl side chain often leads to compounds with high GluN2B affinity [21, 31]. this 4-phenylcyclohexyl moiety was used in the NO_2 derivative **6** and the benzoxazolone **7**. Some modifications led to promising GluN2B affinity (e.g. NO_2 derivative **6** with the 4-phenylcyclohexyl moiety, ketone **9**), but none of these structural variations led to an increased GluN2B inhibition. For the NO_2 derivative **6** and the benzoxazolone **7** the rigid 4-phenylcyclohexyl side chain may contribute to the reduced GluN2B inhibition of these ligands. In conclusion, tetrahydro-3-benzazepine-1,7-diol WMS-1410 (**2**) with 3-fold increased GluN2B inhibitory activity compared to ifenprodil remains the lead compound for future structural modifications.

Acknowledgements

Author Contributions
Nadine Ritter: Recording the TEVC data for compound ds **8**-**10**.
Marvin Korff: Collection of the data; writing the manuscript; analysis of SAR.
Alexander Markus: Synthesis of compound **7**.
Dirk Schepmann: Recording the GluN2B, σ_1 and σ_2 affinity of the ligands.
Julian Schreiber: Recording the TEVC data for compounds **1**-**7**. Docking studies.
Guiscard Seebohm: Supervisor of the project.
Bernhard Wünsch: Supervisor of the project; writing the manuscript.

Funding Sources
This work was supported by the Deutsche Forschungsgemeinschaft (DFG). Funding of the research training group GRK 2515, "Chemical biology of ion channels (Chembion)" is gratefully acknowledged.

Statement of Ethics
Ethics approval is not required since neither animal nor human studies were performed.

Supporting Information
The Supporting Information contains experimental procedures for receptor binding studies and the statistical data analysis of the TEVC experiments.

Disclosure Statement

The authors have no conflicts of interest to declare.

References

1 Danysz W, Parsons CG: Glycine and N-Methyl-D-aspartate receptors: physiological significance and possible therapeutic applications. Pharmacol Rev 1998;50:597–664.
2 Bräuner-Osborne H, Egebjerg J, Nielsen EO, Madsen U, Krogsgaard-Larsen P: Ligands for glutamate receptors: design and therapeutic prospects. J Med Chem 2000;43:2609–2645.
3 Stark H, Reichert U, Graßmann S: Struktur, Funktion Und potentielle therapeutische Bedeutung von NMDA-Rezeptoren, Teil 1. Pharm Unserer Zeit 2000;2:159–166.
4 Papouin T, Ladepeche L, Ruel J, Sacchi S, Labasque M, Hanini M, et al.: Synaptic and extrasynaptic NMDA receptors are gated by different endogenous coagonists. Cell 2012;150:633–646.
5 Chen HV, Lipton SA: The chemical biology of clinically tolerated NMDA receptor antagonists. J Neurochem 2006;97:1611–1626.

6 Zhou X, Hollern D, Liao J, Andrechek E, Wang H: NMDA receptor-mediated excitotoxicity depends on the coactivation of synaptic and extrasynaptic receptors. Cell Death Dis 2013;4:e560.
7 Parsons MP, Raymond LA: Extrasynaptic NMDA Receptor Involvement in Central Nervous System Disorders. Neuron 2014;82:279–293.
8 Liu J, Chang L, Song Y, Li H, Wu Y: The role of NMDA receptors in Alzheimer's disease. Front Neurosci 2019;13:43.
9 Zhang Z, Zhang S, Fu P, Zhang Z, Lin K, Ka-Shun Ko J, et al.: Roles of glutamate receptors in Parkinson's disease. Int J Mol Sci 2019;20:4391.
10 Das J: Repurposing of drugs – The ketamine story. J Med Chem 2020;63:13514–13525.
11 Stark H, Reichert U, Graßmann S: Struktur, Funktion und potentielle therapeutische Bedeutung von NMDA-Rezeptoren, Teil 2. Pharm Unserer Zeit 2000;2:228–236.
12 Paoletti P, Neyton J: NMDA receptor subunits: function and pharmacology. Curr Opin Pharmacol 2007;7:39–47.
13 Paoletti P, Bellone C, Zhou Q: NMDA receptor subunit diversity: impact on receptor properties, synaptic plasticity and disease. Nat Rev 2013;14:383–400.
14 Karakas E, Simorowski N, Furukawa H: Subunit arrangement and phenylethanolamine binding in GluN1/GluN2B NMDA receptors. Nature 2011;475:249–253.
15 Karakas E, Furukawa H: Crystal structure of a heterotetrameric NMDA receptor ion channel. Science 2014;344:992-997.
16 Lee CH, Lü W, Michel JC, Goehring A, Du J, Song X, et al.: NMDA receptor structures reveal subunit arrangement and pore architecture. Nature 2014;511:191–197.
17 Zhu S, Stein RA, Yoshioka C, Lee CH, Goehring A, Mchaourab HS, et al.: Mechanism of NMDA receptor inhibition and activation. Cell 2016;165:704–714.
18 Borza I, Domány G: NR2B selective NMDA antagonists: The evolution of the ifenprodil-type pharmacophore. Curr Top Med Chem 2006;6:687–695.
19 Avenet P, Léonardon J, Besnard F, Graham D, Frost J, Depoortere H, et al.: Antagonist properties of the stereoisomers of ifenprodil at NR1A/NR2B subtypes of the NMDA receptor expressed in *Xenopus* oocytes. Eur J Pharmacol 1996;296:209–213.
20 Williams K: Ifenprodil, a novel NMDA receptor antagonist: site and mechanism of action. Curr Drug Targets 2001;2:285–298.
21 Tewes B, Frehland B, Schepmann D, Robaa D, Uengwetwanit T, Gaube F, et al.:: Enantiomerically pure 2-methyltetrahydro-3-benzazepin-1-ols selectively blocking GluN2B subunit containing N-methyl-D-aspartate receptors. J Med Chem 2015;58:6293–6305.
22 Markus A: Synthese und Struktur-Affinitäts-Beziehungen NR2B-selektiver NMDA-Rezeptorantagonisten mit tricyclischer Oxazolobenzazepinon-Struktur. Dissertation, Münster, 2010.
23 Schepmann D, Frehland B, Lehmkuhl K, Tewes B, Wünsch B: Development of a selective competitive receptor binding assay for the determination of the affinity to NR2B containing NMDA receptors. J Pharm Biomed Anal 2010;53:603–608.
24 Thum S, Schepmann D, Reinoso RF, Alvarez I, Ametamey SM, Wünsch B: Synthesis and pharmacological evaluation of fluorinated benzo 7annulen-7-amines as GluN2B-selective NMDA receptor antagonists. J Labelled Compd Radiopharm 2019;69:354–379.
25 Meyer C, Neue B, Schepmann D, Yanagisawa S, Yamaguchi J, Würthwein EU, et al: Improvement of σ_1 receptor affinity by late-stage C-H-bond arylation of spirocyclic lactones. Bioorg Med Chem 2013;21:1844–1856.
26 Miyata K, Schepmann D, Wünsch B: Synthesis and σ receptor affinity of regioisomeric spirocyclic furopyridines. Eur J Med Chem 2014;83:709–716.
27 Hasebein P, Frehland B, Lehmkuhl K, Fröhlich R, Schepmann D, Wünsch B: Synthesis and pharmacological evaluation of like- and unlike-configured tetrahydro-2-benzazepines with the α-substituted benzyl moiety in the 5-position. Org Biomol Chem 2014;12:5407–5426.
28 DeHaven-Hudkins DL, Fleissner LC, Ford-Rice FY: Characterization of the binding of 3H(+)-pentazocine to σ recognition sites in guinea pig brain. Eur J Pharmacol Mol Pharmacol: 1992;227:371–378.
29 Mach RH, Smith CR, Childers SR: Ibogaine possesses a selective affinity for σ2 receptors. Life Sci 1995;57:PL57–PL62.

30 Schreiber JA, Schepmann D, Frehland B, Thum S, Datunashvili M, Budde T, et al.: A common mechanism allows selective targeting of GluN2B subunit-cont)aining N-methyl-D-aspartate receptors. Commun Biol 2019;2:420–233.
31 Tewes B, Frehland B, Schepmann D, Schmidtke KU, Winckler T, Wünsch B: Conformationally constrained NR2B selective NMDA receptor antagonists derived from ifenprodil: Synthesis and biological evaluation of tetrahydro-3-benzazepine-1,7-diols. Bioorg Med Chem 2010;18:8005–8015.
32 Dey S, Temme L, Schreiber JA, Schepmann D, Frehland B, Lehmkuhl K, et al: Deconstruction – reconstruction approach to analyze the essential structural elements of tetrahydro-3-benzazepine-based antagonists of GluN2B subunit containing NMDA receptors. Eur J Med Chem 2017;138:552–564.
33 Thum S, Schepmann D, Ayet E, Pujol M, Nieto FR, Ametamey SM, et al.: Tetrahydro-3-benzazepines with fluorinated side chains as NMDA and σ_1 receptor antagonists: Synthesis, receptor affinity, selectivity and antiallodynic activity. Eur J Med Chem 2019;177:47–62.
34 Falck E, Begrow F, Verspohl EJ, Wünsch B: Metabolism studies of ifenprodil, a potent GluN2B receptor antagonist. J Pharm Biomed Anal 2014;88:96–105.
35 Falck E, Begrow F, Verspohl EJ, Wünsch B: vitro and *in vivo* biotransformation of WMS-1410, a potent GluN2B selective NMDA receptor antagonist. J Pharm Biomed Anal 2014;94:36–44.
36 Börgel F, Galla F, Lehmkuhl K, Schepmann D, Ametamey SM, Wünsch B: Pharmacokinetic properties of enantiomerically pure GluN2B selective NMDA receptor antagonists with 3-benzazepine scaffold. J Pharm Biomed Anal 2019;172:214–222.
37 Tahar AH, Grégoire L, Darré A, Bélanger N, Meltzer L, Bédard PJ: Effect of a selective glutamate antagonist on l-DOPA-induced dyskinesias in drug-naive parkinsonian monkeys. Neurobiol Dis 2004;15:171–176.
38 Moreau B, Lavielle S, Marquet A: Utilisation du groupe allyle comme groupe protecteur d'amines Application à la synthése de la biotine. Tetrahedron Lett 1977;30: 2591–2594.
39 Shimano M, Matsuo A: Diastereoselective conjugate 1,6-addition of lithium amides to naphthyloxazolines. Mechanistic studies and synthesis of δ-amino acid derivatives. Tetrahedron 1998;54:4787–4810.